THREE NEW SOLAR-POWERED SPECIES OF THE GENUS *PHYLLODESMIUM* EHRENBERG, 1831 (MOLLUSCA: NUDIBRANCHIA: AEOLIDIOIDEA) FROM THE TROPICAL INDO-PACIFIC, WITH ANALYSIS OF THEIR PHOTOSYNTHETIC ACTIVITY AND NOTES ON BIOLOGY

INGO BURGHARDT[1], MICHAEL SCHRÖDL[2] AND HEIKE WÄGELE[3,4]

[1]*Lehrstuhl für Evolutionsökologie und Biodiversität der Tiere, Ruhr-Universität Bochum, Universitätsstr. 150, 44780 Bochum, Germany;*
[2]*Zoologische Staatssammlung München, Münchhausenstr. 21, 81277 München, Germany;*
[3]*Institut für Evolutionsbiologie und Ökologie, Rheinische Friedrich-Wilhelms-Universität, An der Immenburg 1, 53121 Bonn, Germany; and*
[4]*Zoologisches Forschungsmuseum Alexander Koenig, Bonn, Germany*

(Received 16 October 2006; accepted 12 May 2008)

ABSTRACT

Three new *Phyllodesmium* species, *Phyllodesmium lizardensis* n. sp. from Lizard Island (Australia), *P. lembehensis* n. sp. from Sulawesi (Indonesia) and *P. koehleri* n. sp. from the Philippines, are described. *Phyllodesmium lizardensis* n. sp. and *P. lembehensis* n. sp. are associated with octocorals of the family Xeniidae and are similar to other Xeniidae-feeding *Phyllodesmium* species. Nevertheless, unique combinations of cerata morphology and colour, tooth and jaw morphology, the position of the anal papilla, as well as the special digestive glandular branching system within the cerata clearly distinguish these new species from described ones. *Phyllodesmium koehleri* n. sp. probably feeds on octocorals of the genera *Lemnalia* or *Paralemnalia*; it shows a cactus-like cerata morphology that is unique among *Phyllodesmium* species. *In vivo* measurements of photosynthetic activities in *P. lizardensis* n. sp. and *P. lembehensis* n. sp. indicate a symbiotic relationship with zooxanthellae at least for some days. These results are discussed in comparison to the Xeniidae-feeding species *P. jakobsenae* Burghardt & Wägele, 2004 and *P. rudmani* Burghardt & Gosliner, 2006. Histological investigation of the digestive diverticula within the cerata of all new species also suggests a relatively high efficiency of the symbiosis.

INTRODUCTION

So far, 17 species of the genus *Phyllodesmium* Ehrenberg, 1831 (Facelinidae, Aeolidioidea) have been described (see Rudman, 1981, 1991; Baba, 1949, 1991; Avila *et al*., 1998; Ortiz & Gosliner, 2003; Burghardt & Wägele, 2004; Burghardt & Gosliner, 2006). Probably, 10 more species are known from the Indo-West Pacific (www.seaslugforum.net). Thus, compared with other genera of Facelinidae, the genus *Phyllodesmium* is relatively diverse. The species of *Phyllodesmium* are mainly distinguished by different external colour patterns, the shape of the cerata, digestive gland ramification, differences in radular morphology and anal position. The focus of the present study is on the description of three new species of *Phyllodesmium* from different locations in the tropical Indo-West Pacific (Australia, Indonesia and the Philippines). Like all other members of *Phyllodesmium*, the new species appear to feed exclusively on octocorals. Two of the species described herein are specialized in feeding on xeniid corals, while the third feeds on nephtheid corals. Many *Phyllodesmium* species house zooxanthellae inside their digestive glandular cells (Wägele & Johnsen, 2001; Burghardt & Wägele, 2004; Burghardt & Gosliner, 2006). The source of these dinoflagellates of the genus *Symbiodinium* is, as far as we know, solely octocorals. The relationships between the zooxanthellae and *Phyllodesmium* range, depending on the nudibranch species, from uptake with rapid subsequent digestion of the algae to a highly evolved mutualistic symbiosis. Thus, the second aim of the present study is to explore a potential symbiosis of these new species with *Symbiodinium*.

Rudman (1981, 1991) hypothesized a correlation between the grade of branching of the digestive gland and the efficiency of the symbiosis. Species with a higher ramification of the digestive gland (e.g. 'secondary' branching) are assumed to be more derived and adapted to a symbiotic relationship. These assumptions were confirmed by measurements of the photosynthetic activity of the zooxanthellae within different *Phyllodesmium* species (Burghardt & Wägele, 2004; Burghardt *et al*., 2005; Burghardt & Gosliner, 2006; Burghardt, Stemmer & Wägele, 2008). Rudman (1981, 1991) further suggested that species feeding on xeniid corals might be closely related and show a less-developed stage of symbiosis, according to their less-developed digestive glandular structures. The two new species herein described that feed on Xeniidae (*Phyllodesmium lizardensis* n. sp. and *P. lembehensis* n. sp.) were cultivated under starving conditions in aquaria. By applying the pulse amplitude modulated fluorometer (PAM) technology, the photosynthetic activity of their zooxanthellae was measured in order to test Rudman's hypothesis of lower efficiency of the symbiosis.

MATERIAL AND METHODS

Specimens of *Phyllodesmium lizardensis* n. sp. were collected by the first author and colleagues by hand, during two field trips to Lizard Island (Australia) in 2004 and 2005, while snorkelling along reef flats. Individuals of *P. lembehensis* n. sp. were also collected by hand by the first author during a field trip to Sulawesi (Indonesia) in August 2003 while snorkelling. Specimens of

Correspondence: I. Burghardt; e-mail: ingo.burghardt@rub.de

Phyllodesmium koehleri n. sp. were collected by Erwin Köhler during field trips to the Philippines in 2003 and 2005, by hand while diving. For details, see Table 1.

Four specimens of *Phyllodesmium lizardensis* n. sp. and three specimens of *P. lembehensis* n. sp. were kept in aquaria for several days in order to perform starving experiments and to investigate a possible symbiotic relationship with zooxanthellae. *Phyllodesmium lizardensis* n. sp. was kept in aquaria with a flow-through water system under natural moderate light conditions (up to a maximum of *c.* 350 μmol quanta $m^{-2} s^{-1}$ at solar noon) for the whole time of the experiments at the Lizard Island Research Station. The water temperature was approximately 26°C. *Phyllodesmium lembehensis* was kept in an aquarium under natural, moderate, light conditions (in the shade under a roof; up to a maximum of ~400 μmol quanta $m^{-2} s^{-1}$ at solar noon) in Bitung (Lembeh Strait, Sulawesi, Indonesia). Water has been changed daily and the temperature was lying approximately at 27°C. Natural light conditions mean natural light climate conditions in which irradiance, spectral irradiance and photoperiod are driven by the sun's position (sun angle), clouds, the extinction coefficient of water and depth.

A Pulse Amplitude Modulated Fluorometer (Diving-PAM, Walz, Germany) was used to detect *in vivo* photosynthetic activity of zooxanthellae in the investigated specimens of *Phyllodesmium lizardensis* n. sp. and *P. lembehensis* n. sp. by measuring the fluorescence emitted by photosystem II (PSII) of chlorophyll *a*. This allows the distinction between actively photosynthetic zooxanthellae and digested ones inside the nudibranch, and interspecific differences can be detected. The method has already been applied in other opisthobranch species including some *Phyllodesmium* species (Wägele & Johnsen, 2001; Burghardt & Wägele, 2004; Burghardt *et al.*, 2005; Burghardt & Gosliner, 2006). PAM measurements could not be performed on *P. koehleri*, since specimens were preserved directly after collecting.

The PAM comprises a main instrument, a cosine-corrected light collector, and an optic fibre. In all measurements, the optic fibre of the PAM was placed about 0.5 cm from the part of the nudibranch with the highest concentration of zooxanthellae as detected by highest *in vivo* fluorescence – in the investigated species mainly in the upper half of the cerata. Before and between the measurements the slugs were dark-acclimated for 10 min to allow the reaction centres of PS II to recover after light saturation. The settings on the PAM were the same for all measurements, and the voltage of the battery was monitored for all measurements (not dropping below 10 V). Photosynthetic activity is detected by measuring the ground fluorescence of the zooxanthellae inside the nudibranch using a very low light source (F_0 = fluorescence in dark acclimated tissues; F'_0 = fluorescence in actinic light conditions). To analyse the maximum fluorescence and hence the efficiency of photosynthetic activity, a flash of approximately 10,000 μmol quanta $m^{-2} s^{-1}$ for 0.8 s is applied via the optic fibre to shut down reaction centres of PSII (F_m = maximum fluorescence in dark-acclimated tissues during flash; F'_m = maximum fluorescence in light-acclimated tissues during flash). Measurements of the maximum quantum yield of fluorescence emitted by chl *a* PSII ($\varphi_{IIe\text{-}max}$) were taken after dark acclimation. The maximum quantum yield, $\varphi_{IIe\text{-}max}$, defined as

$$\varphi_{IIe\text{-}max} = \frac{(F_m - F_0)}{F_m} \quad (1)$$

was used to investigate the photosynthetic activity of the zooxanthellae in the slugs as a function of time (compare Wägele & Johnsen, 2001; Burghardt & Wägele, 2004; Burghardt *et al.*, 2005; Burghardt & Gosliner, 2006; Burghardt, Stemmer & Wägele, 2008). For the $\varphi_{IIe\text{-}max}$ *vs* time plots (Fig. 9), four specimens of *P. lizardensis* n. sp. and three specimens of *P. lembehensis* n. sp. were measured, beginning on the day of capture.

To obtain photosynthesis *vs* irradiance curves (P–E curves), the same four specimens of *Phyllodesmium lizardensis* n. sp. and three specimens of *P. lembehensis* n. sp. were analysed. The *P–E* curves indicate nonacclimated photosynthetic responses to different light intensities and therefore can indicate differences in the light acclimation abilities of a certain species. The *P–E* curves were obtained using a gradient from low (*c.* 3 μmol quanta $m^{-2} s^{-1}$) to high (*c.* 800 μmol quanta $m^{-2} s^{-1}$) irradiances with 10 min incubation time for each irradiance (eq. 2). The light source was natural sunlight. For the attenuation of different irradiances, spectrally neutral white cotton tissue was used for shading.

Under actinic light conditions, the following equation is used to calculate the operational quantum yield of chl *a* fluorescence (φ_{IIe}):

$$\varphi_{IIe} = \frac{(F'_m - F'_0)}{F'_m} \quad (2)$$

To avoid any impact of light acclimation effects, all measurements of *P–E* curves were performed during the first 3 days after capture of the animals. After the *P vs E* experiment, the specimens were dark acclimated, and then measured again, to test whether *Symbiodinium* regained the maximum fluorescence quantum yield and to ensure that the zooxanthellae inside the animals were not stressed during the experiment and were still active.

The relative electron transfer rate ($P = \varphi_{IIe} \cdot E$), which reports photosynthetic rate, was plotted against irradiance (E) and fitted to eq. 3 (Webb, Newton & Starr, 1974). Hence, the photosynthetic rate (P) and the maximum light utilization coefficient [$\alpha = (\varphi_{IIe} \cdot E) \cdot E^{-1}$] were obtained and the light saturation parameter ($E_k = P_{max} / \alpha$) was calculated.

For the calculations, the following equation was used

$$P = P_{max}(1 - e^{-\alpha \frac{E}{P_{max}}}) \quad (3)$$

where P = photosynthetic rate at a given actinic irradiance, $P = \varphi_{IIe} \cdot E$ where $P = \varphi_{IIe}$ [mol charge separation · mol quanta absorbed^{-1}] · E [μmol quanta $m^{-2} s^{-1}$], P_{max} = maximum photosynthetic rate (same units as P), α = maximum light utilization coefficient [$\alpha = (\varphi_{IIe} \cdot E) \cdot E^{-1}$], φ_{IIe} = operational quantum yield [mol charge separation · mol quanta absorbed^{-1}], $\varphi_{IIe\text{-}max}$ = maximum quantum yield [mol charge separation · mol quanta absorbed^{-1}], E = irradiance (PAR, 400–700 nm; [μmol quanta $m^{-2} s^{-1}$]), $E_k = P_{max}/\alpha$ = light saturation index in μmol quanta $m^{-2} s^{-1}$.

The *P–E* curves and the resulting values (P_{max}, E_k, α) were analysed by the statistics software Kaleidagraph 3.6 (Synergy Software, Reading, USA).

After the long-term experiments, specimens of *Phyllodesmium lizardensis* and *P. lembehensis* n. sp. were preserved in 8% formaldehyde seawater and later transferred to ethanol for dissection and histology. All specimens of *P. koehleri* n. sp. were preserved in 8% formaldehyde seawater directly after capture.

Dissections of the general anatomy were made of five specimens (see Table 1). One specimen of each species and additionally cerata of two more specimens (see Table 1) were embedded in hydroxyethylmethacrylate for histological serial sections (2.5 μm, stained with toluidine blue). Pictures of the histological serial sections were taken with a digital camera (Olympus DP 50) on an Olympus microscope. The hard

Table 1. Investigated specimens of *Phyllodesmium lizardensis* n. sp., *P. lembehensis* n. sp. and *P. koehleri* n. sp.

Phyllodesmium species	No.	Length (living animal) (mm)	Length (pres. animal) (mm)	Locality	Comments	Depository of specimen
P. lizardensis n. sp.	1	45	15	Casuarina Beach, Lizard I., Northern Great Barrier Reef, Australia (GPS 14°40′S 145°28′E) 3 July 2005; ~0.5 m water depth	Dissected; radula; PAM measurements	Paratype: ZSM* Mol 20060654
	2	40	9	Casuarina Beach, Lizard I. 9 July 2005; ~0.5 m water depth	Dissected; PAM measurements	Bochum‡
	3	35	–	Casuarina Beach, Lizard Is. 3 July 2005; ~0.5 m water depth	Histology (whole animal)	Bochum‡
	4	45	16	Loomis Beach, Lizard I., 26 July 2005; ~0.5 m water depth	PAM measurements	Holotype: AMS† C.212810
	5	28	10	Loomis Beach, Lizard I., 28 August 2004; ~0.5 m water depth	Histology (cerata); PAM measurements	Paratype: AMS C.212811
P. lembehensis n. sp.	1	19	6	Lembeh Strait, Sulawesi, dive site 'Awshuck', Indonesia (GPS 01°30′01.5″N 125°14′35.1″E), 2 August 2003; ~0.3 m water depth	PAM measurements	Paratype: ZSM* Mol 20060656
	2	16	5	Lembeh Strait, Sulawesi, 2 August 2003; ~0.3 m water depth	Radula; PAM measurements	Bochum‡
	3	17	–	Lembeh Strait, Sulawesi, 2 August 2003; ~0.3 m water depth	Histology (whole animal); PAM measurements	Bochum‡
	4	21	7	Lembeh Strait, Sulawesi, 2 August 2003; ~0.3 m water depth	Dissected	Paratype: ZSM* Mol 20060656
	5	23	8	Lembeh Strait, Sulawesi, 2 August 2003; ~0.3 m water depth	Dissected	Holotype: ZSM* Mol 20060655
P. koehleri n. sp.	1	44	–	Cabilao I., divesite Busstop, Phlippines, 04.05.03; ~5 m water depth	Histology (whole animal)	Bochum‡
	2	47	13	Cabilao I., divesite 'Busstop', Phlippines, 04.05.03; ~5 m water depth	Histology (cerata); dissected	Paratype: ZSM* Mol 20060657
	3	42	22	Calangaman I. (North Cebu), Philippines, 13 March 2005; ~12 m water depth		Holotype: ZSM* Mol 20060658

*Zoologische Staatssammlung München (Germany).

†Australian Museum, Sydney.

‡Lehrstuhl für Evolutionsökologie und Biodiversität der Tiere, Ruhr-Universität Bochum, Bochum (Germany).

structures of the digestive system (jaws and radula) were prepared for investigations with an SEM (Zeiss DSM 950).

SYSTEMATIC DESCRIPTIONS

Family Facelinidae Bergh in Carus, 1889

Phyllodesmium Ehrenberg, 1831

Type species: *P. hyalinum* Ehrenberg, 1831, by monotypy.

Diagnosis: Following Rudman (1981), members of the genus *Phyllodesmium* are characterized by the following features: cerata slightly or extremely flattened, usually lacking functional cnidosacs and autotomizing readily; ceratal arrangement variable with precardiac arch on each side either single- or double-rowed; postcardiac cerata arranged in single- or double-rowed arches, simple rows, or a mixture of single-rowed arches and simple rows; position of anus cleioproctic, lying in first postcardiac arch or behind first postcardiac row or (in one species) above postcardiac arch; genital opening below anterior limb of right precardiac arch. Oral glands absent, a pair of discrete tubular salivary glands present. Radula formula $n \times 0.1.0$; teeth usually with long pointed central cusp with a lateral flange down each side bearing many denticles or serrations; occasionally serrations strongly developed into long thin tubular denticles, or absent; masticatory process of jaws slightly roughened or developed into strong pointed serrations; reproductive system with single allosperm receptacle and prostate forming gland mass at base of muscular penis. Presently, the genus is only recorded from the Indo-West Pacific, and only known to feed on Alcyonaria (Cnidaria).

Phyllodesmium lizardensis n. sp.

(Figs 1A–F, 3A–D, 6A, 6D, 7A–D, 9, 10D)

Phyllodesmium cf. *hyalinum*—Wägele *et al*., 2006: 57, table I.

Type material: Australian Museum (holotype: C.212810, paratype C.212811); Zoologische Staatssammlung München (ZSM, paratype: ZSM Mol 20060654).

Ethymology: Named after its type locality Lizard Island (Great Barrier Reef, Australia).

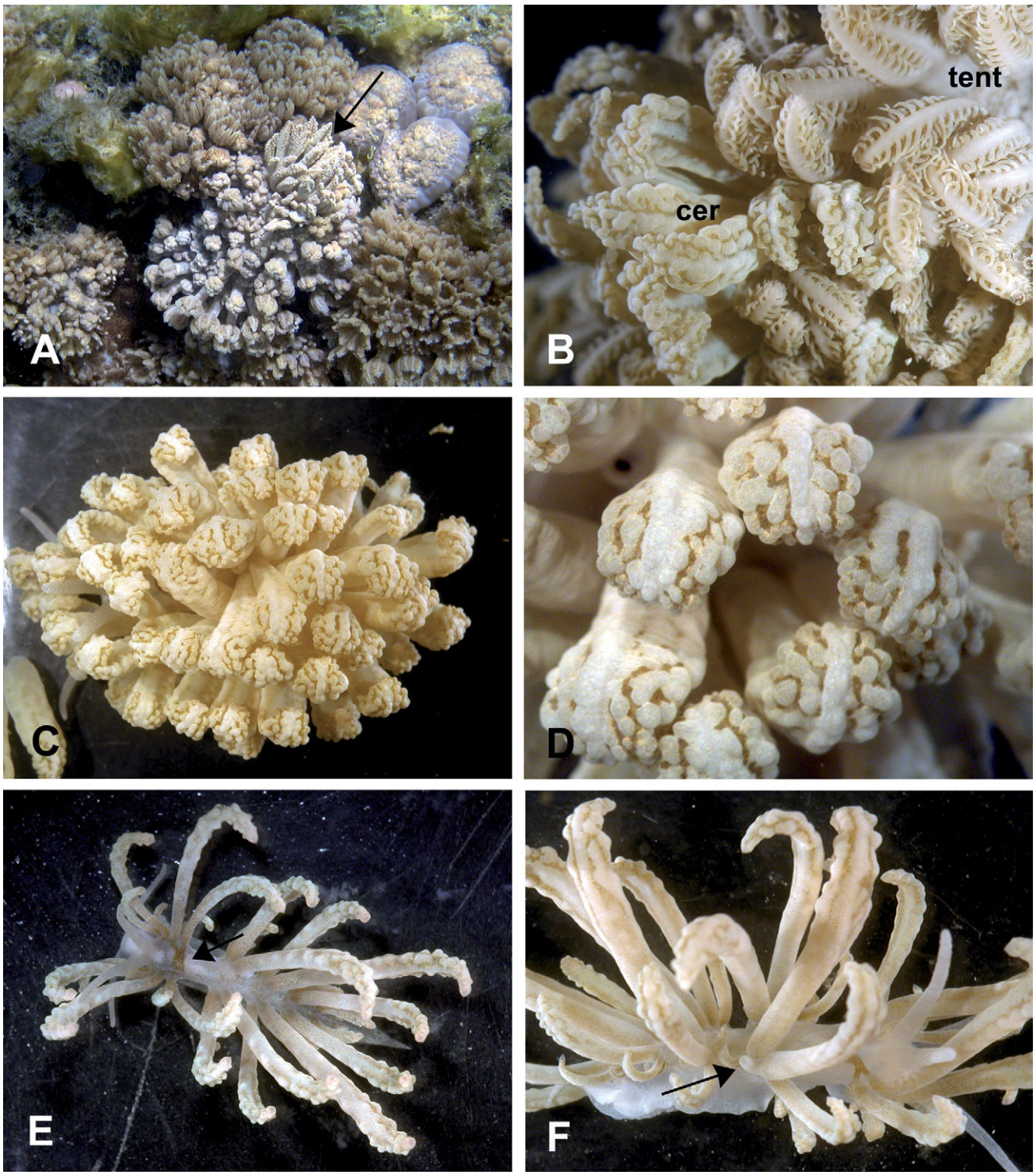

Figure 1. *Phyllodesmium lizardensis* n. sp., living animals. **A.** One specimen (arrow) sitting within xeniid coral colony. **B.** Another specimen, nestled into a xeniid coral colony. The cryptic cerata (left) mimic the coral's tentacles (right) providing good camouflage. **C.** Resting specimen. Note the different appearance compared to moving specimens (**E**). The cerata appear inflated and cover the whole animal. **D.** Magnification of inflated cerata. Note the pustules of the distal ceras part and the brownish coloured (due to zooxanthellae) depressions in between. **E.** Moving specimen. Note the different appearance compared to resting specimens (**C**). Also note the distinct brown digestive glandular branch (arrow) and the distinct area without any cerata between first and second cerata patch. **F.** Position of anus papilla lying within or behind second ceratal row (arrow). Abbreviations: cer, cerata of *P. lizardensis* n. sp.; tent, tentacles of xeniid coral.

Colour and external morphology of living animal: Body of living animals, including oral tentacles, rhinophores, and foot, translucent white. Basic colour of cerata creamish. Right digestive glandular branch distinct due to brown colour (Fig. 1E). Animals elongate, to *c.* 45 mm in length (without cerata), with few short and several very long cerata (longer than rhinophores

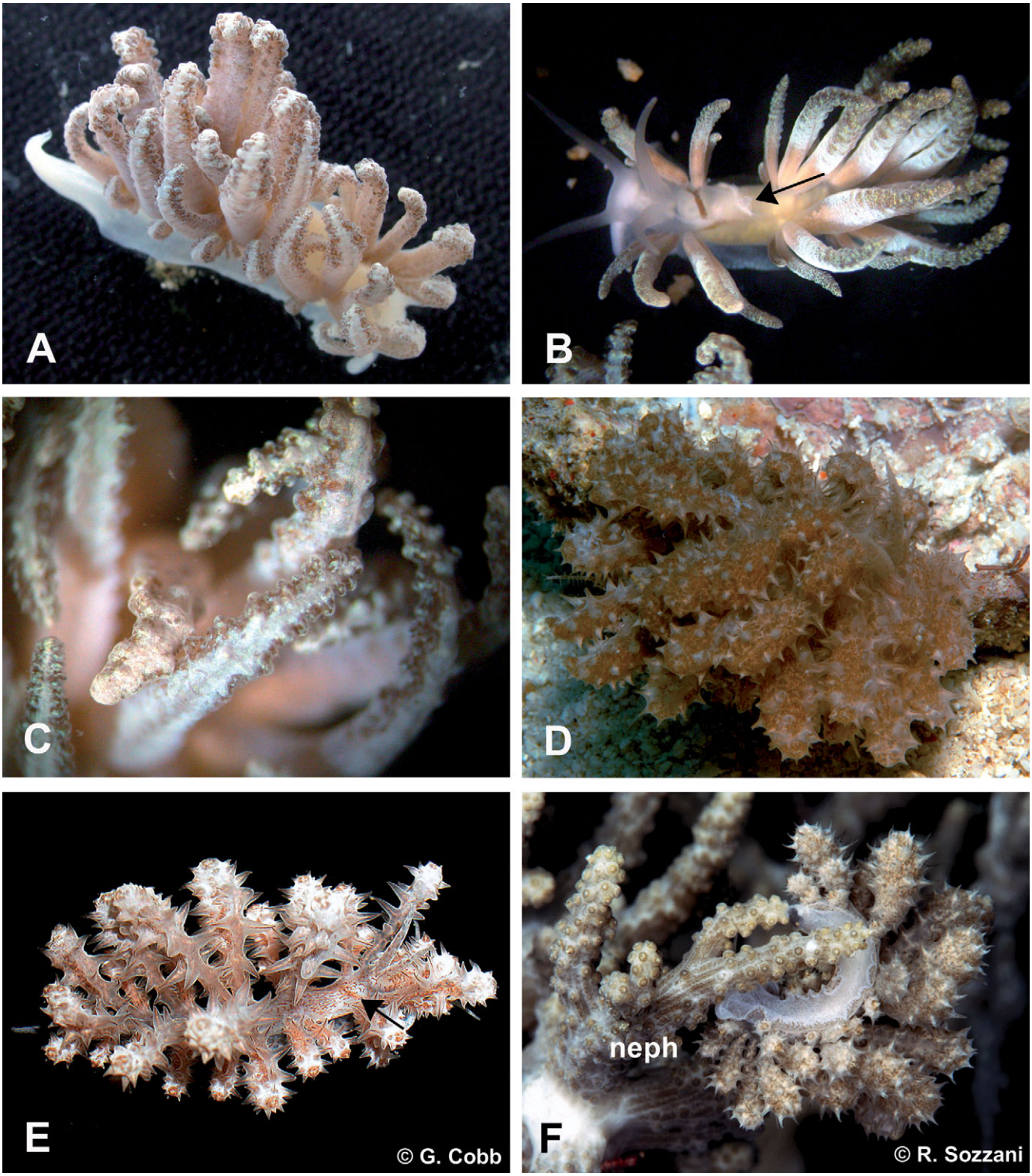

Figure 2. *Phyllodesmium lembehesis* n. sp. (**A–C**) and *P. koehleri* n. sp. (**D–F**), living animals. **A.** Resting specimen of *P. lembehesis* n. sp. Note the densely arranged cerata and the resulting different appearance compared to moving specimens. **B.** Moving specimen of *P. lembehesis* n. sp. Note the distinct brown digestive glandular branch, the dorsal anal papilla (arrow) and the distinct area without any cerata between first and second cerata row. **C.** Magnification of distal ceras part of *P. lembehesis* n. sp. Note the pustules and the brownish edges of the cerata (due to zooxanthellae). **D.** Resting specimen of *P. koehleri* n. sp. Note the densely arranged cerata and the resulting different appearance compared to moving specimens. **E.** Moving specimen of *P. koehleri* n. sp. Note the distinct brown digestive glandular branch (arrow). **F.** *P. koehleri* n. sp. feeding on its probable food coral, belonging to the family Nephtheidae. Note the similarities between cerata of *P. koehleri* n. sp. and parts of the soft coral. Abbreviation: neph, nephtheid soft coral.

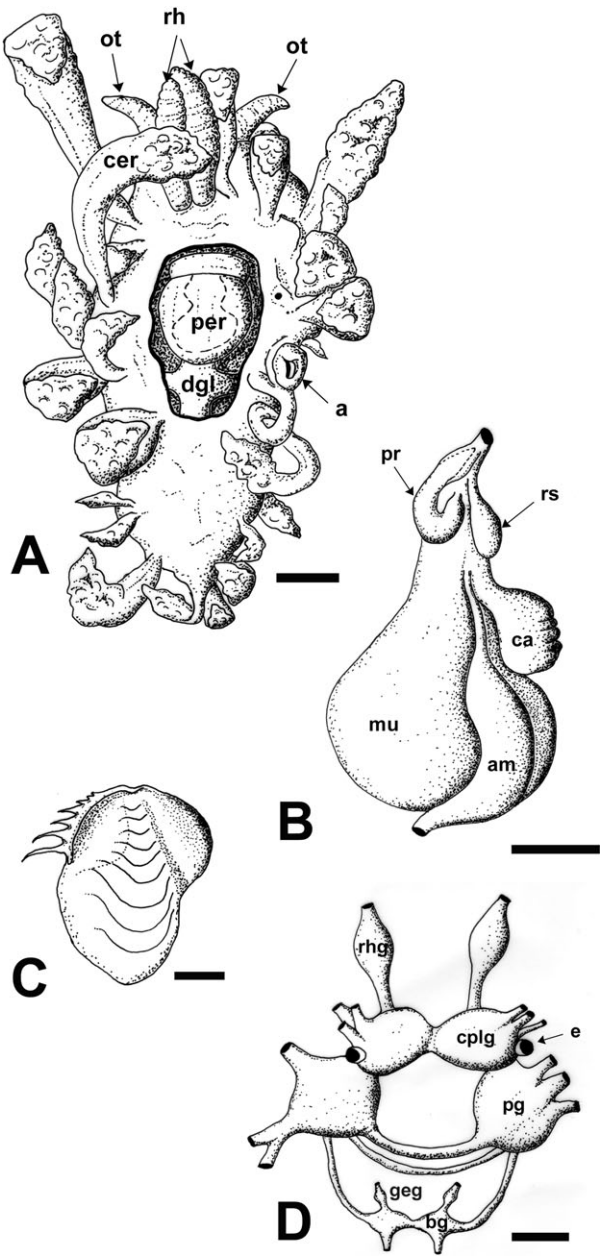

Figure 3. *Phyllodesmium lizardensis* n. sp., morphology. **A.** General outline of organs *in situ*. **B.** Distal genital system. **C.** Right jaw seen from the interior side. **D.** Central nervous system. Abbreviations: a, anal papilla; am, ampulla; bg, buccal ganglion; ca, capsule gland; cer, ceras; cplg, cerebropleural ganglion; dgl, digestive gland; e, eye; geg, gastroesophageal ganglia; mu, mucous gland; ot, oral tentacles; per, pericard; pg, pedal ganglion; pr, prostate; rs, receptaculum seminis; rh, rhinophore; rhg, rhinophoral ganglion. Scale bars: **A** = 1 mm; **B** = 0.5 mm; **C** = 0.5 mm; **D** = 0.5 mm.

and oral tentacles), covering whole notum (Fig. 1C). When crawling, area without any cerata between first and second cerata pads distinct (Fig. 1E). Following pads lying closer to each other. Smooth oral tentacles somewhat longer than slightly wrinkled rhinophores, usually directed more laterally (Fig. 1E, F). Rhinophores similar in shape and surface texture to oral tentacles, standing close together. Both rhinophores and oral tentacles tapering. Anterior foot corners forming only slightly rounded extensions, with some white colouration mainly along anterior edge. Posterior end of foot tapering. Papilliform anus prominent, lying within or behind second incomplete arch (Fig. 1F, arrow). Nephroproct not found.

Cerata (up to 50) clustered in up to five, mainly incomplete arched pads on each body side. Up to six cerata on each pad. First clusters forming distinct arches on each body side, with genital papilla lying beneath right one. Compared to more dorsal ones, lateral cerata in most specimens very small and short (Fig. 1F). Cerata dorso-ventrally flattened and very often broadened in the upper half (Fig. 1C, D). Basal part circular in cross section. Cerata covered with pustules, more prominent ones lying along the edges, mainly in upper half (Fig. 1B–F). Pustules creamish similar to rhachis and base of cerata, with reticulate pattern of brown lines in depressions between pustules (Fig. 1D). Cerata usually partly curled distally, depending on activity state (Fig. 1C–F).

External morphology of preserved animals: Nearly all cerata repelled. No distinct notal rim present. Foot anteriorly without propodial tentacles, posterior part pointed. Oral tentacles slightly wrinkled, slightly shorter than rhinophores. Rhinophores slightly wrinkled and standing close to each other (Fig. 3A). Larger cerata of preserved animals nearly as long as body. Insertion of cerata difficult to see in preserved specimens, clustered in patches or tight arches. Up to six pads on each side, lying opposite to each other. First cerata lateral to rhinophores. Distance between first and second cluster rather long compared to the next pads. Anal papilla dorso-laterally on right side within or behind second cerata patch/row (Fig. 3A). Genital opening below first cerata pad. Whole epidermis composed of specialized vacuolated cells (Fig. 7D).

Central nervous system: Central nervous system behind pharynx. Cerebral and pleural ganglia fused (Fig. 3D). Buccal ganglia lying beneath oesophagus at junction with pharynx. Gastro-oesophageal ganglia present and very small (Fig. 3D). Large rhinophoral ganglion at base of each rhinophore, connected to cerebral ganglion by short connective (Fig. 3D). Eyes situated directly at cerebral ganglia (Fig. 3D). Statocysts lying between cerebropleural and pedal ganglia. Statocysts with few otoconians. Parapedal commissures present. Visceral loop present, but no distinct ganglia on loop visible. For insertion of nerves see Figure 3D.

Digestive system: Oral tube short, leading into bulbous pharynx. Thick layer of oral glands present with subepidermal cells. This layer is thicker and more evident than in *P. lembehensis* n. sp. and *P. koehleri* n. sp. No oral glands with separate ducts present. Two oval jaw plates present (Fig. 3C). Along cutting edge of jaw plates up to seven flattened denticles, getting progressively larger in size (Figs 3C, 6D). Longest denticles about 400 μm in length. Radular formula of one specimen 40 × 0.1.0. Each rhachidian tooth with large (60 μm long) median pointed cusp, slightly arcuated in lateral view (Fig. 6A). Margin of rhachidian with 36–38, relatively short (3–5 μm long), denticles. Salivary glands very difficult to detect in preparation of animal. Efferent duct very thin, without any bulb. Glandular part not observed. Oesophagus forming small loop, widening considerably towards stomach. Entrances into stomach and digestive gland not visible, due to huge amount of an unknown substance in whole middle part of digestive tract. Interior of oesophagus with specialized vacuolated epithelium. Right and left anterior digestive glandular branch starting above entrance of oesophagus and leading to first ceratal pads on both sides. Right duct brown, differing in colour compared to all other main digestive glandular ducts, which are translucent to slightly brownish (Fig. 1E). One main duct leading to posterior part of body with opposite lying ducts leading into posterior cerata pads. Intestine starting next to oesophagus and anterior digestive glandular branches, leading on right side to anus.

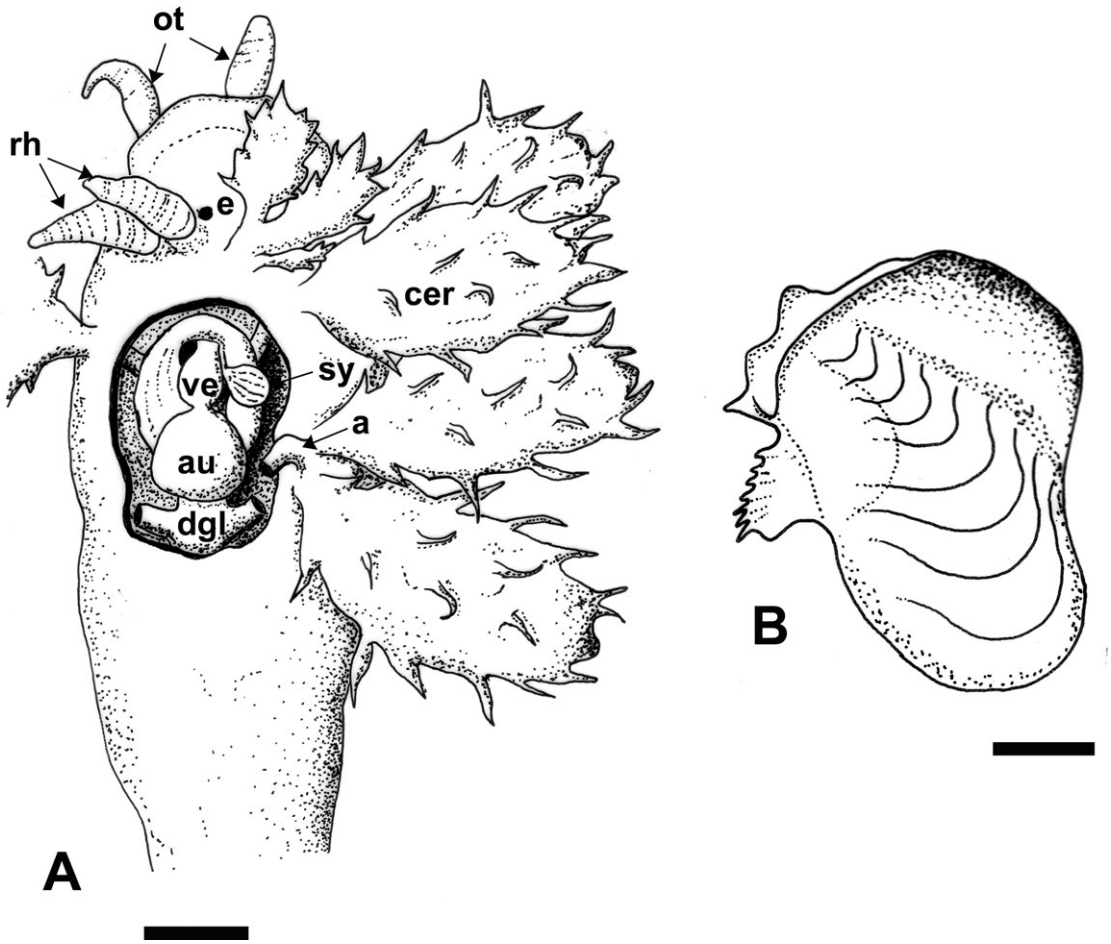

Figure 4. *Phyllodesmium koehleri* n. sp., morphology. **A.** *G*eneral outline of organs *in situ*. **B.** Right jaw seen from the interior side. Abbreviations: a, anal papilla; au, auricle; cer, ceras; dgl, digestive gland; e, eye; ot, oral tentacles; rh, rhinophore; sy, syrinx; ve, ventricle. Scale bars: **A** = 1.5 mm; **B** = 0.5 mm.

Intestine with specialized vacuolated epithelium and in loop of intestine large typhlosole is present.

Digestive gland in cerata: One central narrow digestive gland duct extending into each ceras. Duct regularly constricted. Especially in apical broadened part of ceras, central duct ramifying in primary and secondary branches, latter radiating towards ceratal wall (Fig. 7A, B). Each secondary branch terminating close to ceratal wall. Sac-like structures of secondary digestive glandular branches not present. On the side of flattened part of ceras which is not exposed to light, secondary branches concentrated only at margin of each ceras. Light orientated side of each ceras densely packed with branches directly beneath ceratal wall. Zooxanthellae present in digestive glandular cells, in lumen and in epithelium of these branches (Fig. 7A–C). Cnidosac of large and small cerata with cells each containing one large vacuole (Fig. 7D). No cnidocysts observed in these cells. Distinct muscular layer around cnidosac present (Fig. 7D).

Circulatory and excretory system: Syrinx large, inside highly folded, opening ventrally into pericardium on anterior right side next to ventricle. Kidney elongate, extending mainly from syrinx posterior to anus. Nephroproct not found. Pericardium with distinct ventricle lying dorsally between first and second ceratal pad. Atrium lying behind ventricle, both arranged in longitudinal direction (Fig. 3A).

Reproductive system: Gonad follicles forming floccular mass in posterior part of body. Gonad reaching into anterior third of ventral visceral cavity. Male and female follicles separated. Distal genital system occupying whole anterior part of visceral cavity. Gonoduct with banana-shaped ampulla (Fig. 3B). Mucous gland very large and distinct (Fig. 3B). To right of mucous gland, yellowish hyaline capsule or membrane gland of smaller size present. Transition of mucous gland into distal oviduct not distinguishable, as is opening into atrium. Capsule/membrane gland opening close to entrance of ampulla but rather far back from joined genital opening. Close to genital opening, elongate receptaculum seminis entering atrium close to oviduct opening. Connection of ampulla to vas deferens probably near to atrium. Vas deferens very short, thick, opening into small penial sheath. Penis papilliform. Atrium elongate and large.

Distribution: Only known from two localities around Lizard Island.

Remarks: The type locality (Loomis Reef, Lizard Island) of *P. lizardensis* n. sp. is a shallow coral reef fringed by large sandy areas. Most specimens were found in depths between 0.3 and 1 m. Water temperature at locality was approximately 25–26°C (July–August). Many specimens were found nestled inside large colonies of xeniid corals that were attached to a plastic pipe (Fig. 1A), close to Casuarina Beach (Lizard

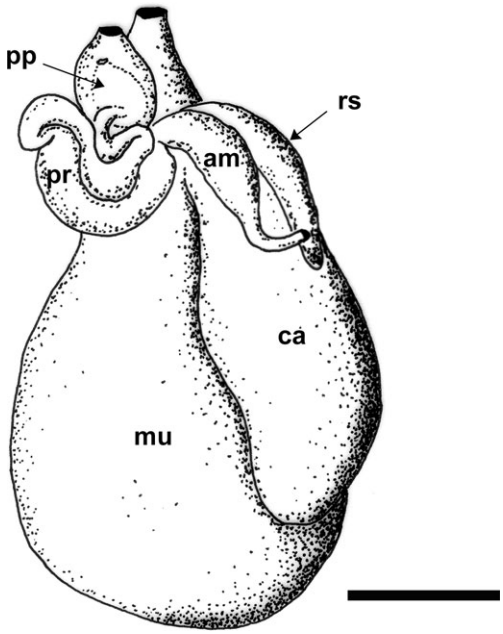

Figure 5. *Phyllodesmium lembehensis* n. sp., distal genital system. Abbreviations: am, ampulla; ca, capsule gland; mu, mucous gland; pp, penis papilla; pr, prostate; rs, receptaculum seminis. Scale bar: 0.5 mm.

Island). None of the specimens of *P. lizardensis* n. sp. were found outside the corals. When sitting on the soft coral, the bodies of the slugs were not visible, only the cerata extended slightly beyond the tentacles of the corals (Fig. 1A). The animals are very well camouflaged, the cerata mimic parts of the tentacles in colour and shape (Fig. 1A, B). Similar to other Xeniidae-feeding congeners, *P. lizardensis* n. sp. mimics the shadows between the pinnules of coral tentacles (Fig. 1B). Observations on *P. lizardensis* n. sp. in the aquarium revealed differences in appearance based on different activity states; when crawling the body of *P. lizardensis* n. sp. is visible and the cerata appear slender and elongated (Fig. 1E), while resting, especially the upper parts of the cerata broaden, inflate and partly curl inwards. In this state, the cerata cover the whole notum (Fig. 1C). Diurnal behaviour like in *P. jakobsenae* (see Burghardt & Wägele, 2004) could not be observed, although most specimens of *P. lizardensis* n. sp. remained more or less inactive during extremely high irradiances (e.g. at solar noon). Several specimens autotomized some of their cerata upon disturbance, a behaviour typical for *Phyllodesmium*. Detached cerata exuded a sticky secretion and moved for some minutes, similar to observations in the other recently described Xeniidae-feeding species *P. jakobsenae* and *P. rudmani*. Some specimens of *P. lizardensis* n. sp. laid spawn masses, especially after disturbance. The spawn mass is a whitish ribbon-like cord of about 32 mm in diameter, with egg capsules arranged in a line.

***Phyllodesmium lembehensis* n. sp.**

(Figs 2A–C, 5, 6B, E, 7E, F, 8A, B, 9, 10C)

Type material: Zoologische Staatssammlung München (holotype: 20060655; paratype: ZSM Mol 20060656).

Ethymology: Named after its type locality Lembeh Strait between Sulawesi and Lembeh Island (Indonesia).

Colour and external morphology of living animal: Body of living animals, including oral tentacles, rhinophores and foot translucent white (Fig. 2A, B). Basic colour of cerata creamish. Right digestive glandular branch distinct due to brown colour (Fig. 2B). Animals elongate, up to approximately 23 mm in length (without cerata), with few short and several long cerata (partly longer than rhinophores and oral tentacles), covering whole notum when resting (Fig. 2A). When crawling, distinct area without any cerata can be observed between first and second ceratal patches (Fig. 2B). Second and following patches lying closer to each other. Smooth oral tentacles somewhat longer than smooth rhinophores, usually slightly directed more laterally. Rhinophores standing close together, similar in shape and surface texture to oral tentacles. Both rhinophores and oral tentacles tapering. Anterior foot angular, with some white colouration mainly along anterior edge (Fig. 2B). Posterior end of foot tapering. Papilliform anus prominent, lying dorsally between first and second arch (Fig. 2B). Nephroproct not observed.

Cerata (35–41) clustered in up to five single, mainly incomplete arches or rows. Up to five cerata on each pad. First cluster forming distinct row. Compared to more dorsal ones, lateral cerata very small and short (Fig. 2A). Cerata dorsoventrally flattened, narrowing in upper half (Fig. 2A). Basal part oval in cross section. Upper half of spatulate, arrowhead-shaped cerata very nodulose, especially along edges (Fig. 2A, C); nodules irregulary arranged. Creamish colour of basal ceras part extenting into rhachis (until apex of ceras). Edges of nodulose distal part of ceras brownish (Fig. 2C). Apex of cerata blunt. Cerata usually partly curled inwards distally, depending on activity state (Fig. 2A, B).

External morphology of preserved animals: Both specimens heavily contracted, heads and tail bent dorsally. Artificial swellings filled with viscera on left body side. Smaller specimen (7 mm) with larger cerata expelled, larger one (8 mm) with large cerata in situ. No distinct notal rim present. Foot bilabiate, lips well developed. Propodial tentacles short, oral tentacles wrinkled, with well-developed lateral groove. Oral tentacles slightly longer than evenly wrinkled rhinophores, latter standing close to each other. First cerata lateral or slightly anterior to rhinophores. Up to five rows or patches of cerata on each side, lying opposite to each other. Distance between first and second patch rather long compared to next patches. Anal papilla dorsally, between first and second cerata patch. Genital opening not found. Whole epidermis composed of specialized vacuolated cells (Fig. 7F).

Central nervous system: Central nervous system behind pharynx, very similar to the other new species described herein.

Digestive system: Oral tube short, subepithelial oral glandular follicles detected by histology. Two oval-shaped jaw plates. Along cutting edge of jaw plates up to eight delicate denticles present, their size only slightly largening towards end of masticatory process (Fig. 6E). Longest denticles about 200 μm in length. Radular formula of one specimen 35 × 0.1.0. Each rhachidian tooth with large (50 μm long) median pointed cusp, slightly arcuated in lateral view (Fig. 6B). Margin of rhachidian with about 36 to 41 relatively short (5 to 7 μm long) denticles. Pharynx bulbous, long radular sac protruding posteroventrally. Thin-walled oesophagus emerging posterodorsally from pharynx. Stomach with specialized vacuolated cells. Stomach elongate. Right and left anterior digestive glandular branches starting above entrance of oesophagus and leading to first cerata pads on both sides. Right duct brown even in preserved specimens, therefore differing from all other main digestive glandular ducts, with translucent to slightly brownish colour (Fig. 2B). Posterior main duct leading to posterior part of body with opposite lying ducts entering into posterior cerata pads. Intestine emerging anterodextrally, running posterior to

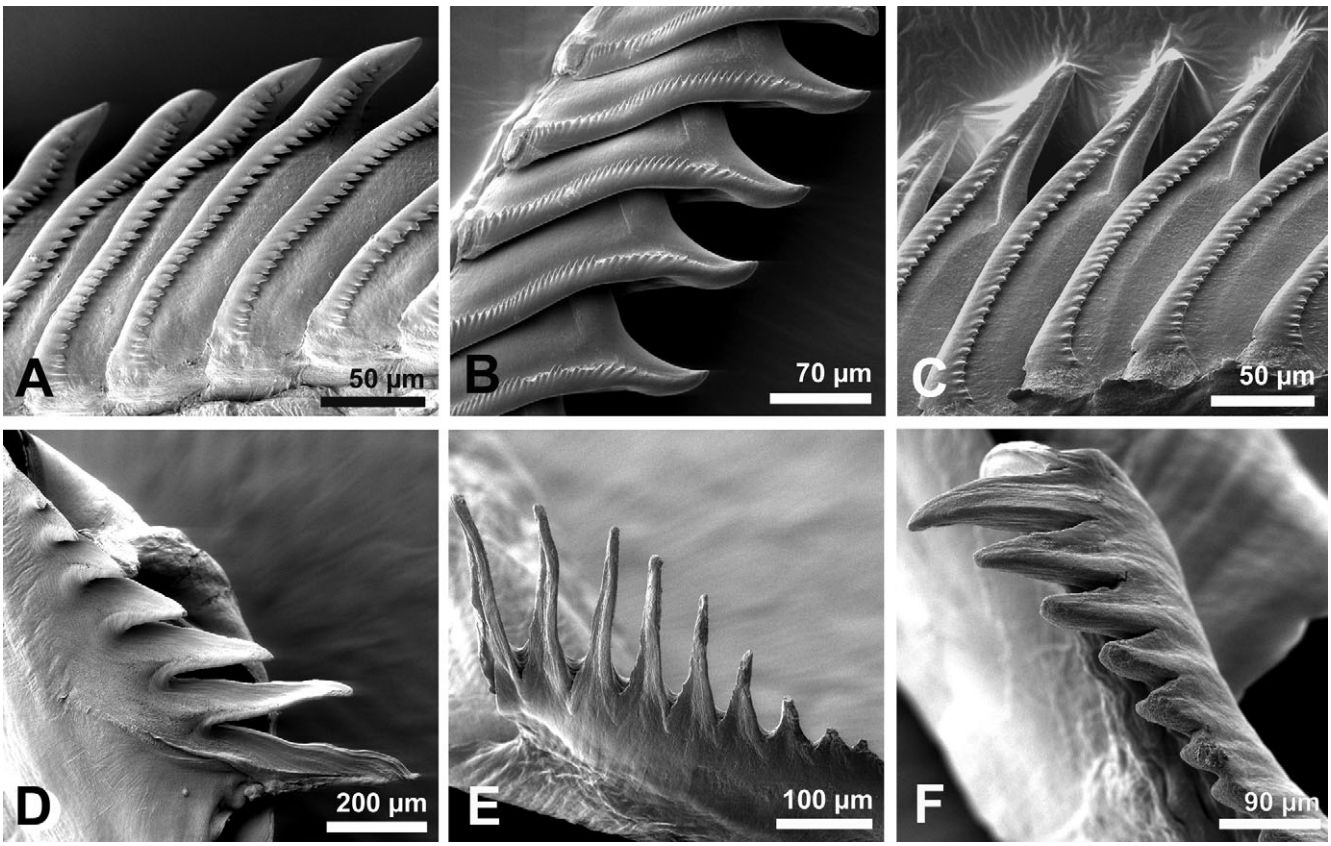

Figure 6. *Phyllodesmium lizardensis* n. sp. (**A, D**), *P. lembehensis* n. sp. (**B, E**) and *P. koehleri* n. sp. (**C, F**), hard structures in digestive system. **A.** Distal part of radula of *P. lizardensis* n. sp. **B.** Distal part of radula of *P. lembehensis* n. sp. **C.** Distal part of radula of *P. koehleri* n. sp. Note the prominent ridge along the median cusp. **D.** Denticles of the jaw of *P. lizardensis* n. sp. Note the flattened denticles. **E.** Denticles of the jaw of *P. lembehensis* n. sp. Note the delicate denticles. **F.** Denticles of the jaw of *P. koehleri* n. sp. Note the compact and strong denticles.

dorsally situated anal papilla. Typhlosole is present in intestine.

Digestive gland in cerata: One central narrow digestive gland duct extending through each ceras (Fig. 7E). Especially in apical, broadened part, central duct ramifying in primary branches, radiating towards ceratal wall (Fig. 7E). Sac-like structures of primary digestive glandular branches not present. Ceratal nodules partly filled with chambers of digestive gland (Fig. 8A). Zooxanthellae present in lumen of digestive gland as well as in digestive glandular cells, of branches in cerata and in chambers (Figs 7E–F, 8A). Dividing zooxanthellae can be detected (Fig. 7F). Cnidosac of large and small cerata with cells each containing one large vacuole (Fig. 8B). No contents observed in these cells. Distinct muscular layer around cnidosac present (Fig. 8D).

Circulatory and excretory system: Heart lying in anterior third of body with atrium posterior to muscular ventricle. Syrinx and kidney in usual position. Nephropore slightly anterior to anus.

Reproductive system: Reproductive system of androdiaulic type with vas deferens separated from female gonoducts (Fig. 5). Male and female follicles separated. Gonad follicles forming a layer filling most of body cavity posterior to pharynx. Distal genital system limited to anterior part of visceral cavity. Hermaphroditic duct widening into relatively small, sausage-shaped ampulla (Fig. 5). Postampullary gonoduct very short. Vas deferens immediately widening into tube-like, prostatic portion with loops attached to each other by connective tissue (Fig. 5). Distal vas deferens muscular, narrower and short. Penial papilla quite large, bluntly conical. Female gland mass large and elongated with large mucous gland and a smaller probably capsule gland connected distally. Elongated allosperm receptacle connected to distal nidamental glands close to insertion of short oviduct.

Distribution: Only known from the type locality in Lembeh Strait, Sulawesi.

Remarks: The type locality ('Awshuck', Lembeh Strait, Sulawesi) of *P. lembehensis* n. sp. is a patchy reef, surrounded by large areas of black volcanic sand. All specimens were sitting in colonies of xeniid corals that covered a dead coral bommie in ~0.3 m depth.

None of the specimens of *P. lembehensis* n. sp. were found outside the corals. Similar to *P. lizardensis* n. sp. and all other Xeniidae-feeding *Phyllodesmium* species, specimens of *P. lembehensis* n. sp. are very well camouflaged, the cerata mimic parts of the coral tentacles in colour and shape (Fig. 2A). With the brownish markings on the cerata (areas with high concentration of zooxanthellae) *P. lembehensis* n. sp. mimics the zooxanthellate parts of the host coral tentacles (Fig. 2A). Individuals of *P. lembehensis* n. sp. and *P. lizardensis* n. sp. have not been found together on the same colonies of the xeniid coral, thus a possible sympatric distribution on the same species of Xeniidae, and therefore sharing the same food source, has yet to be clarified.

Individuals of *P. lembehensis* n. sp. enlarge their cerata and hold them close together while resting (Fig. 2A), shading the rest of the body. Diurnal behaviour as in *P. jakobsenae* (see Burghardt & Wägele, 2004) could not be observed, although

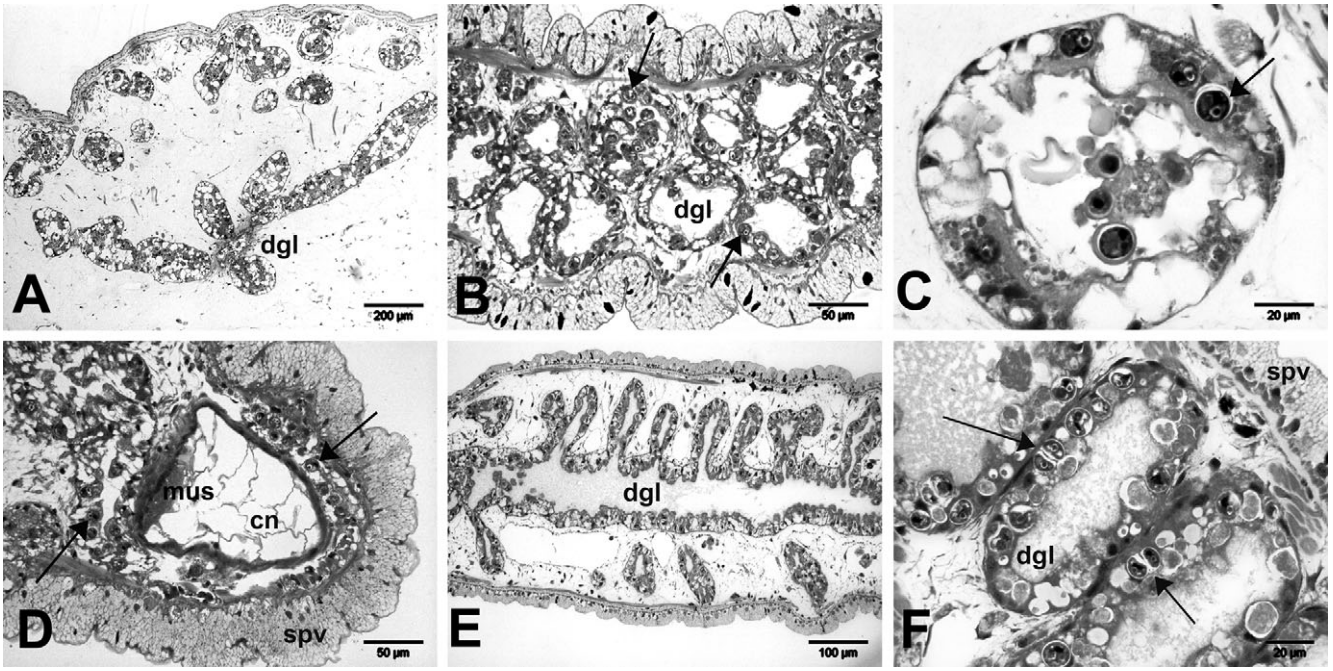

Figure 7. *Phyllodesmium lizardensis* n. sp. (**A–D**) and *P. lembehensis* n. sp. (**E–F**), histology of the digestive gland. **A.** Transversal section: ducts of the digestive gland inside ceras of *P. lizardensis* n. sp. Note the secondary branching grade of the digestive gland. **B.** Longitudinal section: digestive gland within ceras of *P. lizardensis* n. sp. Note the zooxanthellae inside epithelium and lumen of digestive glandular branches. **C.** Magnification of section through digestive glandular branch inside ceras of *P. lizardensis* n. sp. Note the zooxanthellae inside epithelium and lumen of digestive glandular branches. **D.** Longitudinal section: cnidosac inside ceras of *P. lizardensis* n. sp. with cells containing one large vacuole. Note the absence of functional nematocysts, the distinct muscular layer around the cnidosac and the epidermis composed of specialized vacuolated cells. **E.** Longitudinal section through ceras of *P. lembehensis* n. sp. showing primarily branched digestive gland. **F.** Section through digestive glandular ducts of *P. lembehensis* n. sp. Note the dividing zooxanthellae (arrow). Abbreviations: cn, cnidosac; dgl, digestive glandular branches; mus, muscular layer; spv, specialized vacuolated cells. Arrows: Zooxanthellae in digestive gland.

most specimens remained more or less inactive during extremely high irradiances (e.g. at solar noon), similar to *P. lizardensis* n. sp. Several specimens autotomized some of their cerata during disturbance, a behaviour typical for *Phyllodesmium*. As in many other *Phyllodesmium* species, detached cerata exuded a sticky secretion and moved for some minutes.

Phyllodesmium koehleri n. sp.

(Figs 2D–F, 4A, B, 6C, F, 8C–F)

Phyllodesmium sp. 1 Bolland, 2005.
Phyllodesmium sp. 2 Barrett & Barrett, 2004. Sozzani, 2004.
Phyllodesmium sp. 3 Cobb, 2004.

Type material: Zoologische Staatssammlung München (holotype: ZSM Mol 20060658; paratype: ZSM Mol 20060657).

Ethymology: Dedicated to Erwin Köhler, a passionate diver and underwater photographer, who supported us by collecting different *Phyllodesmium* species.

Colour and external morphology of living animal: Body of living animals, including oral tentacles, rhinophores and foot translucent white (Fig. 2E, F). Right digestive glandular branch dark brown (Fig. 2E). Animals elongate, up to approximately 56 mm (Bolland, 2006) in length (without cerata), with few short and several very long cerata (longer than rhinophores and oral tentacles), covering whole notum when resting (Fig. 2D). Smooth oral tentacles somewhat longer than smooth to slightly wrinkled rhinophores, usually directed more laterally. Rhinophores similar in shape to oral tentacles, standing close together. Both rhinophores and oral tentacles tapering. Anterior foot angular. Posterior end of foot tapering to thin line (Fig. 2E). Papilliform anus prominent and long, dorso-laterally of second cerata pad. Nephroproct not observed.

Up to six cerata arranged in five different clusters on each side. First cluster forming a distinct row on each side, with genital papilla lying beneath right one. Compared to more dorsal cerata, lateral ones smaller and shorter (Fig. 2F). Cerata spoon-like, flattened with concave and convex side, broadening in upper half (Fig. 2D–F). Basal part circular to oval in cross section. Cerata covered with large spiny tubercles, these more elongate along cerata edges (Fig. 2D–F). Apex of cerata clubbed and blunt. Cerata never curled. Brownish digestive gland shining through transparent body wall of cerata, giving some specimens a rather brownish colour (Fig. 2D).

External morphology of preserved animals: No distinct notal rim present. Foot anteriorly without propodial tentacles, posterior part pointed. Oral tentacles slightly annulated due to preservation. Rhinophores slightly wrinkled, standing close to each other, somewhat longer than oral tentacles (Fig. 4A). Up to five pads/rows of cerata on each side, lying opposite to each other. First cerata lateral or slightly anterior to rhinophores. Distance between first and second cluster as long as between all other pads. Anal papilla dorsolateral of second ceratal pad (Fig. 4A). Genital papilla lying beneath first ceratal cluster. Whole epidermis composed of specialized vacuolated cells (Fig. 8D).

Central nervous system: Central nervous system behind pharynx, very similar to all described *Phyllodesmium* species.

Digestive system: Oral tube short, large subepithelial oral glandular follicles detected by histology. Oral tube leading into bulbous pharynx. Along cutting edge of oval shaped jaw plates up to seven strong denticles present, getting progressively

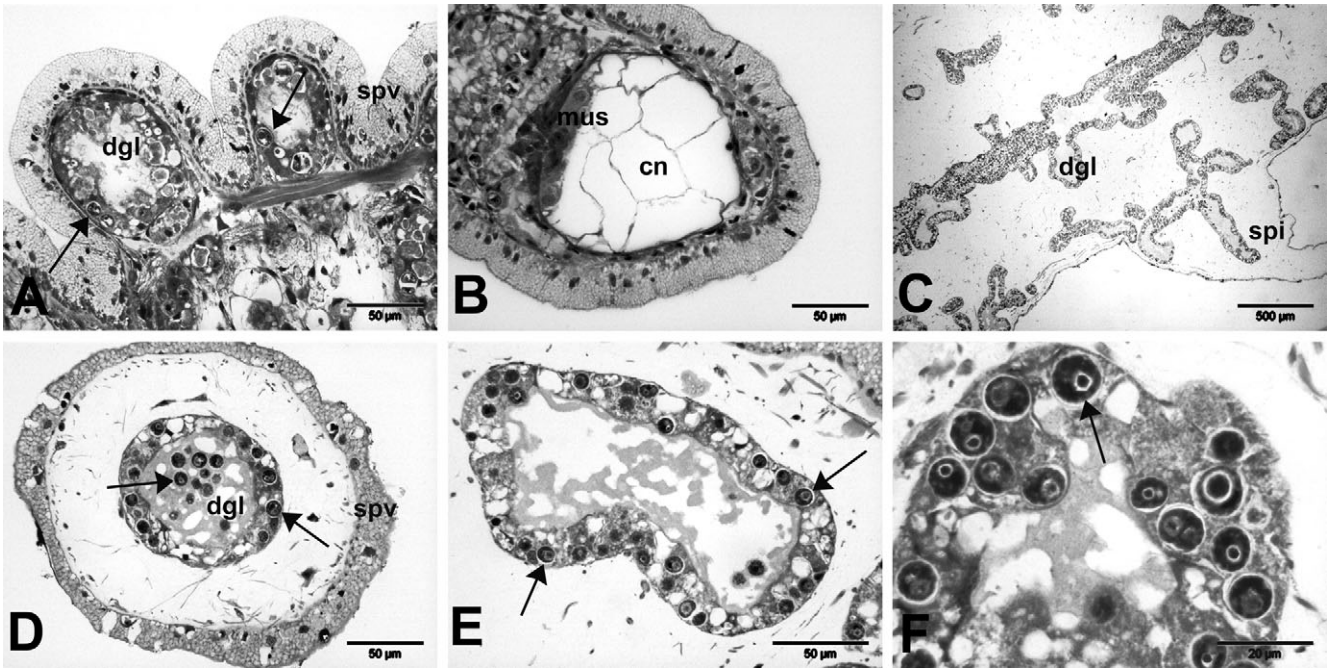

Figure 8. *Phyllodesmium lembehensis* n. sp. (**A–B**) and *P. koehleri* n. sp. (**C–F**), histology of the digestive gland. **A.** Nodules of the cerata of *P. lembehensis* n. sp. filled out with chambers of the digestive gland. Note the zooxanthellae inside the digestive glandular epithelium and the epidermis composed of specialized vacuolated cells. **B.** Longitudinal section: cnidosac inside ceras of *P. lembehensis* n. sp. with cells containing one large vacuole. Note the absence of functional nematocysts, the distinct muscular layer around the cnidosac and the epidermis composed of specialized vacuolated cells. **C.** Longitudinal section: ducts of the digestive gland inside ceras of *P. koehleri* n. sp. Note the secondary branching grade of the digestive gland. **D.** Transversal section: spiny tubercle on ceras of *P. koehleri* n. sp. Note the single duct of the digestive gland with incorporated zoxanthellae (inside the epithelium and lumen) and the epidermis composed of specialized vacuolated cells. **E.** Section through a digestive glandular branch of *P. koehleri* n. sp. Note the numerous zooxanthellae inside the epithelium. **F.** Magnification of a section through a digestive glandular branch of *P. koehleri* n. sp. Abbreviations: cn, cnidosac; dgl, digestive glandular branches; mus, muscular layer; spi, spiny tubercle of cerata; spv, specialized vacuolated cells. Arrows: Zooxanthellae in digestive gland.

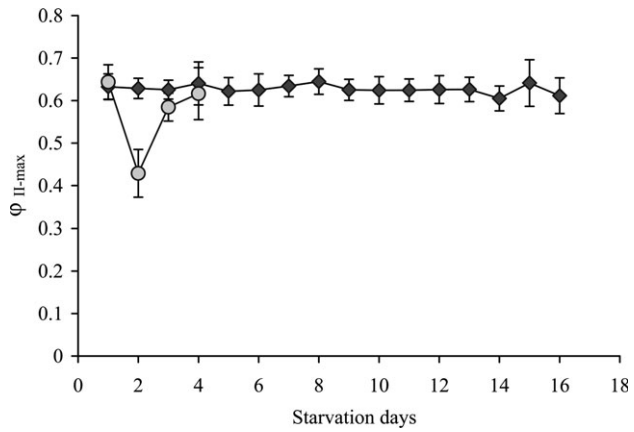

Figure 9. Daily mean values of $\varphi_{\text{IIe-max}}$ of four specimens of *Phyllodesmium lizardensis* n. sp. and of three specimens of *P. lembehensis* n. sp. *vs* starvation days. Of each specimen, four measurements (*P. lizardensis* n. sp.) respectively five measurements (*P. lembehensis* n. sp.) were taken every day. For daily mean values of each specimen see Table 4. Bars indicate the standard deviation (see also Table 4). Individuals of *P. lembehensis* n. sp. were not distinguished. Note the dramatic decrease of the values of *P. lembehensis* n. sp. on starvation day 2 (due to an accidental overexposure of the animals to high irradiances) and the following recovery of the values. Dark grey diamonds: *P. lizardensis* n. sp.; light grey circles: *P. lembehensis* n. sp.

larger in size (Figs 4B, 6F). Longest denticles about 180 μm in length. Radular formula of one specimen $25 \times 0.1.0$. Each rhachidian tooth with large (75 μm long) median pointed and straight cusp, strengthened by a prominent ridge (Fig. 6C). Margin of rhachidian with about 28–31 relatively short (2–5 μm long) denticles. Oesophagus with specialized vacuolated cells. Entrance into stomach not visible. Right and left anterior digestive glandular branch starting above entrance of oesophagus and leading to first ceratal pads on both sides. Right duct brown, therefore differing in colour compared to other slightly brownish main digestive glandular ducts (Fig. 2E). Posterior main duct leading to posterior part of body with opposite lying ducts leading into posterior ceratal pads. Intestine emerging anterodextrally, running posterior to anal papilla. Typhlosole present in intestine.

Digestive gland in cerata: One central narrow digestive gland duct extending through each ceras (Fig. 8C). Central duct ramifying in primary and secondary branches, latter radiating towards ceratal wall (Fig. 8C). Each secondary branch terminating close to ceratal wall. Single branches of the digestive gland reaching into spiny tubercles of the cerata, also visible in living animals (Figs 2E, 8D). Sac-like structures of secondary digestive glandular branches not present. Zooxanthellae present in cells of digestive glandular branches as well as in lumen (Fig. 8D–F). Lumen of branches often filled with amorphous material. Cnidosac of large and small cerata with cells each containing one large vacuole. No contents observed in these cells. Distinct muscular layer present around cnidosac.

Circulatory and excretory system: Syrinx large, highly folded inside, opening ventrally into pericard on anterior right side next to ventricle. Pericard with distinct ventricle lying dorsally between first and second ceratal pads. Atrium lying behind ventricle, both arranged in longitudinal direction (Fig. 4A).

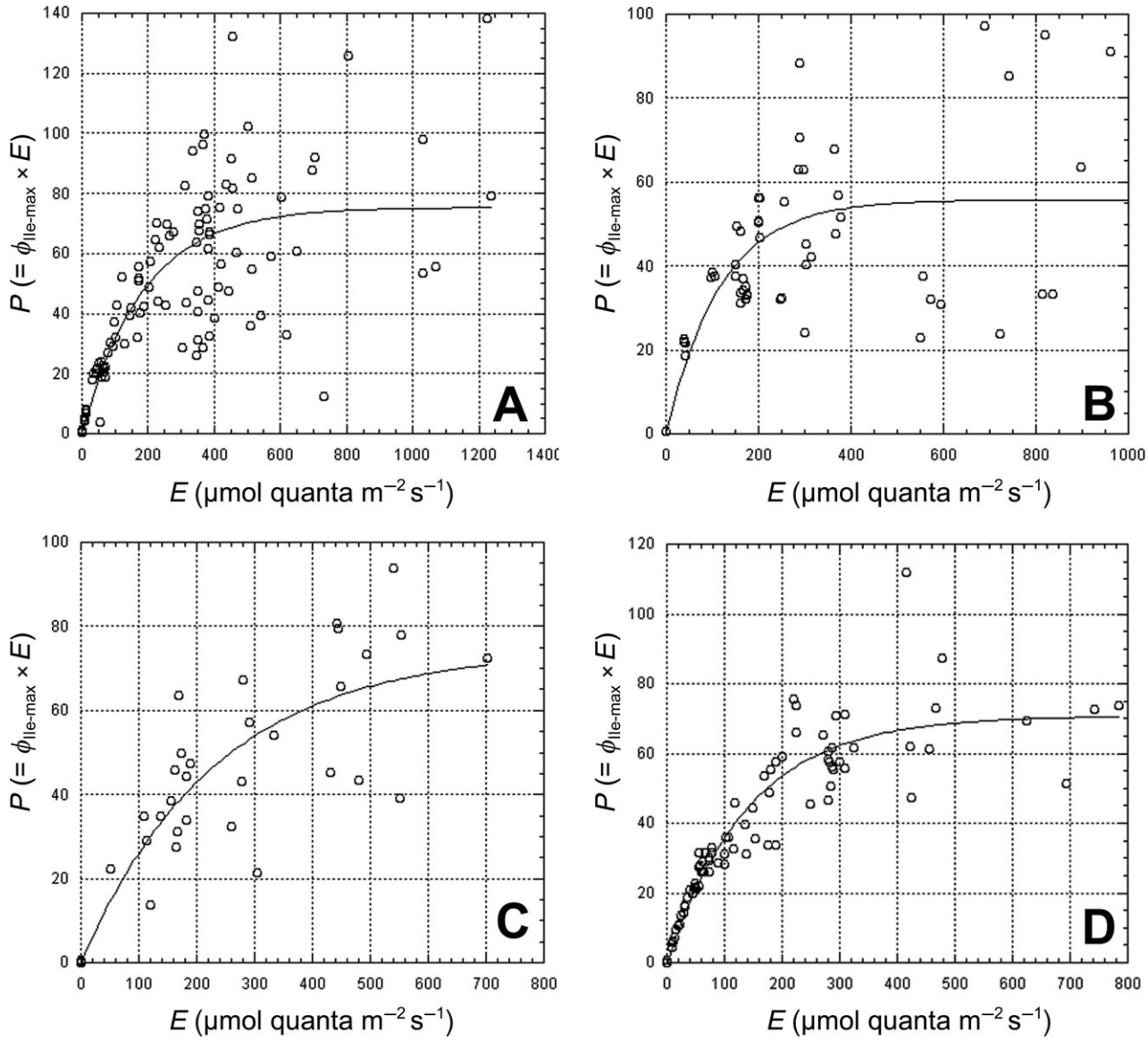

Figure 10. Photosynthetic rate ($P = \varphi_{IIe} \times E$, *y*-axis) *vs* irradiance [*E*; (μmol quanta $m^{-2}\,s^{-1}$), *x*-axis] of *Phyllodesmium jakobsenae*, *P. rudmani*, *P. lizardensis* n. sp. and *P. lembehensis* n. sp. **A.** *P. jakobsenae*. **B.** *P. rudmani*. **C.** *P. lembehensis* n. sp. **D.** *P. lizardensis* n. sp. Note different scales for *P* and *E*.

Reproductive system: Reproductive system of androdiaulic type. Gonad follicles forming floccular mass in posterior part of body. Gonad reaching into anterior third of ventral visceral cavity. Male and female follicles separate. Distal genital system occupying whole anterior part of visceral cavity. General outline of genital system difficult to interpret by macroscopic dissection due to hyaline and hardened structure in the viscera. Following description bases on histological as well as macroscopic investigations. Gonoduct with ampulla lying interiorly and not externally of nidamental glands. Mucous gland very large. Smaller capsule and membrane gland present. Close to genital opening, roundish receptaculum seminis inserting together with oviduct. The receptaculum seminis was not observed in macroscopic investigation, but histological investigation revealed its position within the notum wall. Vas deferens long, thick with prostatic epithelium, opening into penial sheath. Penis papilliform. Atrium not present, oviduct and penis sheath opening separately.

Distribution: Records of *P. koehleri* n. sp. exist from Old Woman Island, Mooloolaba, Australia (Cobb, 2004); Okinawa, Japan (Bolland, 2005); Sulawesi, Indonesia (Sozzani, 2004) and New Britain, Papua New Guinea (Barrett & Barrett, 2004).

RESULTS

Measurements of photosynthetic activity

PSII maximum quantum yield vs time-curves ($\varphi_{IIe\text{-}max} - T$ curves): In Figure 8, the daily mean values of the maximum fluorescence yield ($\varphi_{IIe\text{-}max}$) of four specimens of *Phyllodesmium lizardensis* n. sp. and three specimens of *P. lembehensis* n. sp. (Fig. 9) are plotted *vs* the number of cultivation days under starving conditions in the aquarium. The mean values of $\varphi_{IIe\text{-}max}$ of the four specimens of *P. lizardensis* n. sp. fluctuated slightly, but stayed on a high level (between 0.6 and 0.7) for the whole time of the experiments (Fig. 9; see also Table 4). The mean value of $\varphi_{IIe\text{-}max}$ of the three specimens of *P. lembehensis* n. sp. is 0.644 on the day of capture, decreasing dramatically 1 day later to a mean value of 0.429, and afterwards increasing again to a

Table 2. Comparison of relevant external and anatomical features of known *Phyllodesmium* species with *P. lizardensis* n. sp., *P. lembehensis* n. sp. and *P. koehleri* n. sp. (in bold).

Phyllodesmium species	Characters								
	1	2	3	4	5	6	7	8	9
P. briareum (Bergh, 1896)	+	−	+	−	+	+	−	−	−
P. crypticum Rudman, 1981	+	+	+	+	−	−	−	−	+
P. colemani Rudman, 1991	+	−	+	+	+	+	+	−	−
P. guamensis Avila *et al.*, 1998	+	−	+	+	+	−	−	−	−
P. horridum (Macnae, 1954)	−	−	+	−	−	−	+	−	−
P. hyalinum Ehrenbergh, 1831	+	+	+	+	+	−	+	+	+
P. iriomotense Baba, 1991	−	−	+	−	−	−	−	−	−
P. jakobsenae Burghardt & Wägele, 2004	+	+	+	+	+	+	−	+	+
P. kabiranum Baba, 1991	+	−	+	+	+	−	+	−	−
P. koehleri n. sp.	**+**	**+**	**+**	**+**	**+**	−	−	**+**	−
P. lembehensis n. sp.	**+**	**+**	**+**	**+**	−	−	−	**+**	**+**
P. lizardensis n. sp.	**+**	**+**	**+**	**+**	**+**	−	−	−	**+**
P. longicirrum (Bergh, 1905)	+	−	−	+	+	+	−	−	−
P. macphersonae (Burn, 1962)	+	−	+	−	+	+	−	−	−
P. magnum Rudman, 1991	+	−	−	+	+	+	−	−	−
P. opalescens Rudman, 1991	−	−	+	−	−	−	+	−	−
P. parangatum Ortiz & Gosliner, 2003	+	−	+	+	+	−	−	−	−
P. pecten Rudman, 1981	+	+	+	+	−	−	−	−	+
P. poindimiei (Risbec, 1928)	−	−	+	−	−	−	−	−	−
P. rudmani Burghardt & Gosliner, 2006	+	+	+	−	+	+	+	−	+
P. serratum (Baba, 1949)	−	−	+	−	−	−	−	−	−

Numbers refer to different characters: 1, zooxanthellae incorporated; 2, presence of strong serrations/denticles on the jaws; 3, presence of well-developed rows of denticles on the teeth of the radula; 4, flattened cerata; 5, branching of digestive gland inside cerata at least secondary; 6, presence of sacs at the ends of the fine branches of the digestive gland for storing of zooxanthellae; 7, presence of white patches/pigmentation on body; 8, anal papilla lying dorsally; 9, feeding on xeniid soft corals. + yes/present; − no/absent.

Table 3. Photosynthetic characteristics of the Xeniidae-feeding *Phyllodesmium* species *P. jakobsenae*, *P. lembehensis* n. sp., *P. lizardensis* n. sp. and *P. rudmani*, based on measurements with a Diving-PAM and resulting photosynthesis *vs* irradiance curves (*P–E* curves)

Phyllodesmium species	α	P_{max} (μmol quanta/ $m^{-1}\,s^{-1}$)	E_k (μmol quanta/ $m^{-1}\,s^{-2}$)	Water depth (m)
P. jakobsenae	0.41	75	186	0.3–0.5
P. lembehensis n. sp.	0.32	74	231	0.2–0.3
P. lizardensis n. sp.	0.50	71	142	0.3–1
P. rudmani	0.47	56	118	0.5–1

Values calculated by the statistics software Kaleidagraph 3.6.

α, maximum light utilization coefficient; P_{max}, maximum photosynthetic rate; E_k, light saturation index.

mean value of 0.616 on cultivation day 4 (Fig. 9; see also Table 4).

Photosynthesis vs irradiance curves (P–E curves): Figure 10 shows the photosynthetic rates of four *Phyllodesmium* species feeding on members of the Xeniidae: *P. lembehensis* n. sp., *P. lizardensis* n. sp. and for comparison *P. jakobsenae* and *P. rudmani*, plotted *vs* the irradiance (see also Burghardt & Wägele, 2004; Burghardt & Gosliner, 2006). Specimens of the latter two species were cultivated and measured under almost the same conditions like *P. lembehensis* (under natural moderate light conditions: up to a maximum of ~400 μmol quanta $m^{-2}\,s^{-1}$ at solar noon, 27°C water temperature, up to 3 days after capture). The corresponding values (α, E_k and P_{max}), calculated by Kaleidagraph 3.6, can be seen in Table 3. The maximum light utilization coefficient values (α) of *P. jakobsenae* (0.41) and *P. rudmani* (0.47) are comparably low, but similar to each other. Compared to these two species, the α-value of *P. lizardensis* n. sp. (0.5) is slightly higher, the one of *P. lembehensis* n. sp. (0.32) is lower. The maximum photosynthetic rate (P_{max}) values of *P. jakobsenae* (75 μmol quanta/$m^{-1}\,s^{-2}$), *P. lembehensis* n. sp. (74 μmol quanta/$m^{-1}\,s^{-2}$) and *P. lizardensis* n. sp. (71 μmol quanta/$m^{-1}\,s^{-2}$) are similar, whereas these values are lower in *P. rudmani* (56 μmol quanta/$m^{-1}\,s^{-2}$).

Phyllodesmium rudmani also has the lowest index (E_k value) for light saturation (118 μmol quanta/$m^{-1}\,s^{-2}$), whereas the values of *P. jakobsenae* (186 μmol quanta/$m^{-1}\,s^{-2}$), *P. lembehensis* n. sp. (231 μmol quanta/$m^{-1}\,s^{-2}$) and *P. lizardensis* n. sp. (142 μmol quanta/$m^{-1}\,s^{-2}$) are relatively high.

DISCUSSION

Taxonomy

According to the features outlined by Rudman (1981), the three new species can be assigned to the genus *Phyllodesmium*: reproductive system is similar to all other described species of *Phyllodesmium*; shape of the radular tooth and jaws very similar; replacement of the cnidosac by a terminal sac without cnides; easily autotomizing cerata that wriggle and exude a sticky secretion when autotomized. Additionally, the new species also feed on alcyonarian octocorals (Xeniidae respectively *Paralemnalia* sp. or *Lemnalia* sp.). Rudman (1981) stated that the absence of oral glands is a generic feature. This has to be changed in the light of recent findings in *Phyllodesmium jakobsenae* and in the new species of the present study. In all newly described species, oral glands are present and form thick layers surrounding the oral tube rather than separate organs with a distinct duct. Furthermore, no salivary glands were found. The older descriptions concerning presence of salivary glands and absence of oral glands should be reinvestigated.

Phyllodesmium species that are found exclusively on xeniid corals can be distinguished from all other species of the genus by morphological, anatomical and ecological differences (see Table 2). The former are characterized by a distinct area without any cerata between first and second cerata clusters (Figs 1E, 2B; see also Burghardt & Wägele, 2004; Burghardt & Gosliner, 2006), the latter show branches of the digestive gland, which pervade the whole body and lie between the viscera. Xeniid feeders only show branches in the cerata.

Externally, the two xeniid feeders described here, *Phyllodesmium lizardensis* n. sp. and *P. lembehensis* n. sp., are similar to the other five Xeniidae-feeding species of *Phyllodesmium*: *P. crypticum* Rudman, 1981, *P. hyalinum* Ehrenberg, 1831, *P. pecten* Rudman, 1981, *P. jakobsenae* Burghardt & Wägele, 2004, and *P. rudmani* Burghardt & Gosliner, 2006. They all mimic the tentacles of the corals in one or other way and are very cryptic. Most sophisticated is *P. rudmani*, in which the tips of the cerata mimic the tentacles of the polyps. All seven Xeniidae feeders, including the new species, show strong denticles on the masticatory border of the jaws. This has been discussed by Rudman (1981) for *P. crypticum*, *P. hyalinum* and *P. pecten* as a feature connected with feeding on xeniid corals and separating these from other *Phyllodesmium* species, including *P. koehleri* n. sp. Two other Xeniidae feeders are extremely

Table 4. Daily mean values and standard deviation of the four specimens of *Phyllodesmium lizardensis* n. sp. and the three specimens of *P. lembehensis* n. sp. measured with the Diving-PAM.

Specimen	Time series														
P. lizardensis															
No. 1	Day	1	2	3	4	5	6	7	8	9	10	11	12	13	14	15	16
	Mean	0.621	0.622	0.635	0.665	0.623	0.63	0.614	0.638	0.627	0.617	0.634	0.617	0.625	0.615	0.629	0.62
	SD	0.016	0.016	0.009	0.047	0.018	0.011	0.022	0.008	0.009	0.051	0.019	0.011	0.038	0.038	0.024	0.029
No. 2	Day	1	2	3	4	5	6	7	8	9	10	11	12	13	14	15	16
	Mean	0.664	0.627	0.616	0.63	0.603	0.607	0.648	0.64	0.637	0.647	0.627	0.633	0.626	0.613	0.684	615
	SD	0.047	0.04	0.036	0.05	0.021	0.015	0.012	0.009	0.019	0.017	0.034	0.034	0.03	0.026	0.056	0.016
No. 4	Day	1	2	3	4	5	6	7	8	9	10	11	12	13	14	15	16
	Mean	0.625	0.631	0.62	0.678	0.633	0.652	0.655	0.656	0.627	0.61	0.625	0.635	0.631	0.595	0.606	0.638
	SD	0.012	0.01	0.014	0.012	0.057	0.049	0.007	0.042	0.04	0.027	0.034	0.025	0.028	0.036	0.073	0.062
No. 5	Day	1	2	3	4	5	6	7	8	9	10	11	12	13	14	15	16
	Mean	0.627	0.627	0.633	0.588	0.627	0.61	0.62	0.644	0.609	0.628	0.608	0.618	0.622	0.597	0.646	0.578
	SD	0.033	0.019	0.023	0.036	0.022	0.052	0.025	0.047	0.023	0.031	0.016	0.055	0.029	0.02	0.04	0.047
P. lembehensis																	
No. 1–3	Day	1	2	3	4												
	Mean	0.644	0.429	0.585	0.616												
	SD	0.04	0.56	0.032	0.061												

These data are the base for Figure 9. For information on individuals see Table 1.

similar in shape to *Phyllodesmium lizardensis* n. sp., namely *P. hyalinum* and *P. crypticum*. Despite the similarities, *P. lizardensis* n. sp. can be clearly distinguished from these by several characters: the anterior foot corners of *P. lizardensis* sp. nov. form only slightly rounded extensions, whereas *P. crypticum* has distinct tentacular processes. The cerata of *P. lizardensis* n. sp. are dorsoventrally flattened and covered by irregularly lying pustules in the upper part whereas smooth and circular in cross section at the base (Fig. 1C–F). In contrast, the cerata of *P. crypticum* are quadrangular in cross section and covered with nodules that are mainly arranged in rows, especially along the edges. The cerata of *P. hyalinum* are slightly flattened, smooth at the base and only slightly nodulose in the apical part. *Phyllodesmium rudmani*, with cerata shaped like polyps, shows a unique morphology of the cerata compared to *P. lizardensis* n. sp.; the cerata of *P. rudmani* are roundish in cross section and look like a whole closed coral polyp whereas the cerata of *P. lizardensis* are more flattened and look like the tentacles of a coral polyp.

The cerata of *P. lizardensis* sp. nov. are arranged in single rows, the long anal papilla lies within or behind the second ceratal row (Fig. 1F). In contrast, the cerata of *P. hyalinum* are arranged in double rows and the anus papilla is situated dorsally of the second ceratal row. The coarse serration of the cutting edge of the jaw plate in *P. lizardensis* n. sp. is weaker and the denticles of the jaws appear stronger but more flattened than in *P. crypticum* (Fig. 6D). Additionally, the teeth of the cutting edge of the jaw plates progressively increase in size, whereas the denticles of *P. crypticum* are irregular in length. The denticles of *P. jakobsenae* have deep depressions and are clog-shaped and therefore easily distinguishable from the jaws of *P. lizardensis* n. sp. The number of denticles on the radular teeth is much lower in *P. lizardensis* n. sp. (<38 denticles) compared to *P. hyalinum* (up to 56 denticles). The branching of the digestive gland is secondary in *P. lizardensis* n. sp. (Fig. 7A), whereas in *P. crypticum* and *P. pecten* it is only primary.

Phyllodesmium lembehensis n. sp. also shares some similarities with *P. crypticum* and *P. hyalinum*, but can also be distinguished from these and other Xeniidae-feeding species by a combination of different characters. Similar to *P. crypticum*, the cerata of *P. lembehensis* n. sp. are very nodulose, but the nodules of the latter are arranged in an irregular pattern, especially in the upper part of the ceras (see Fig. 2A, C), whereas in *P. crypticum* they occur on the whole ceras and are arranged in rows. In contrast to *P. crypticum*, the anterior foot corners of *P. lembehensis* n. sp. only form slightly rounded extensions.

Phyllodesmium lembehensis n. sp. (Fig. 2B), *P. hyalinum* and *P. jakobsenae* share a more dorsally situated anal papilla than the other Xeniidae feeders. In contrast to the strongly dorsoventrally flattened cerata of *P. jakobsenae* and *P. lizardensis* sp. nov., the spatulate and only slightly flattened cerata of *P. lembehensis* sp. nov. taper towards their apex (Fig. 2A). The branching grade of the digestive gland inside the cerata is primary in *P. lembehensis* n. sp. and therefore less ramified than in *P. hyalinum*, *P. jakobsenae* and *P. lizardensis* (Fig. 7E). The ceratal pads of *P. hyalinum* are arranged in double rows, whereas in *P. lembehensis* n. sp., similar to *P. lizardensis* n. sp., they are arranged in single rows. The denticles of the jaw plates of *P. lembehensis* n. sp. appear much more delicate and slender compared to other Xeniidae-feeding species (Fig. 6E).

Phyllodesmium koehleri n. sp. differs from all other described *Phyllodesmium* species in its food preferences. This species seems to be specialized on members of the Nephtyidae, probably *Paralemnalia* or *Lemnalia* (Sozzani, 2004; identification of corals by P. Alderslade, personal communication). The spoon-like spiny cerata of *P. koehleri* n. sp. mimic parts of these soft corals (Fig. 2D–F) and clearly distinguish *P. koehleri* n. sp. from all other congeners. The colour of the cerata probably again

originates from the zooxanthellae extracted from the same coral. In contrast to many other *Phyllodesmium* species, the cerata are never curled in the upper part. Similar to all non-Xeniidae-feeding *Phyllodesmium* species described so far, *P. koehleri* n. sp. has branches of the digestive gland within the body (Fig. 2E). As in Xeniidae-feeding species, the right digestive glandular branch is distinct due to brown colour (Fig. 2E) and the very long anal papilla lies rather dorsally. Unusual are the strong denticles along the edges of the jaw plates (Fig. 6F), a character assumed to be typical for Xeniidae feeders. The rhachidian teeth of the radula are strengthened with a distinct prominent ridge (Fig. 6C).

Mutualistic symbiosis

As already suggested by Rudman (1991) for other zooxanthellate aeolids, we assume that housing zooxanthellae has advantages for the species described here. The cerata mimicking the polyps of the coral in colour and shape indicate crypsis as an important evolutionary trait. The availability of additional nutrients (photosynthetic products) is a second advantage.

All Xeniidae-feeding species described earlier (*Phyllodesmium crypticum*, *P. hyalinum*, *P. jakobsenae*, *P. pecten* and *P. rudmani*) are already known to have a symbiotic relationship with zooxanthellae, albeit with different efficiencies (Rudman, 1981, 1991; Burghardt & Wägele, 2004; Burghardt & Gosliner, 2006). The dorso-ventrally flattened cerata of many species increase the surface area exposed to light and therefore increase the availability of light for the zooxanthellae. Rudman (1991) outlined an evolutionary scenario of the symbiotic relationship within the genus *Phyllodesmium*, based on branching patterns of the digestive gland. According to him, a higher branching grade of the digestive gland is correlated with a more effective symbiosis, and the Xeniidae-feeding species known at that time (*P. crypticum*, *P. hyalinum* and *P. pecten*) represent an early stage in the evolution of zooxanthellae symbiosis with only a short-term retention of zooxanthellae. In contrast to this assumption, Burghardt & Wägele (2004) have shown that the Xeniidae-feeding *P. jakobsenae* has flattened cerata and exhibits a relatively high grade of digestive glandular branching, which can be termed 'secondary' according to the terminology of Rudman (1981, 1991). Additionally, *P. jakobsenae* has sac-like structures for storing zooxanthellae at the end of the fine branches. These sac-like structures are mainly situated in the dorsal, light-exposed side of the ceras. All these features indicate a very well established mutualistic symbiosis, similar to that described for *P. macphersonae*, *P. briareum* and *P. colemani*, species that feed on other octocorals (Burghardt, Stemmer & Wägele, 2008). Our results on the Xeniidae-feeding species *Phyllodesmium lizardensis* n. sp. also indicate an effective symbiosis with zooxanthellae. The branching grade of the digestive gland is at least secondary (Fig. 7A), but sac-like structures at the end of the fine branches of the digestive gland as an adaptation for storing zooxanthellae are missing. This might indicate a less-developed symbiosis in comparison to, for example, *P. jakobsenae*.

Measurements with the Diving-PAM clearly indicate that *Symbiodinium* cells are alive and photosynthetically active within *P. lizardensis* n. sp. The maximum yield values ($\varphi_{\mathrm{IIe\text{-}max}}$) stayed at a high level for the whole time, even after 16 days of starvation (Fig. 9), indicating a stable symbiotic relationship between this species and the zooxanthellae (at least for the time of the experiments) and no high turnover of zooxanthellae. The slope of the photosynthesis *vs* irradiance curves (P–E curves) and the resulting photosynthetic characteristics give evidence for functional chloroplasts (Fig. 10D). Compared to the values of other solar-powered nudibranchs (see Burghardt *et al*., 2005; Burghardt & Wägele, 2006), the values of α (maximum light utilization coefficient), E_k (light saturation index) and P_{max} (maximum photosynthetic rate) are relatively low, but similar to other Xeniidae-feeding *Phyllodesmium* species (see Table 3). The low E_k and P_{max} values indicate shade acclimated/adapted (*Symbiodinium*) cells that in fact are efficient in light harvesting and the high values indicate the opposite. Interspecific differences in nudibranchs might be due to different *Symbiodinium* strains/ecotypes that are different light sensitive or due to light acclimation of the same strain (Burghardt & Wägele, 2004; Burghardt *et al*., 2005).

In the other new Xeniidae-feeding species, *Phyllodesmium lembehensis* n. sp., the branching grade of the digestive gland is less developed (only primary, Fig. 7E) than in *P. jakobsenae* or *P. lizardensis* n. sp., but chambers of the digestive gland with incorporated zooxanthellae in the nodules of the cerata are present (similar to *P. jakobsenae*) and expose the zooxanthellae optimally to the light (Fig. 8A). Dividing zooxanthellae within this species confirm this assumption (Fig. 7F). The high $\varphi_{\mathrm{IIe\text{-}max}}$ values between 0.6 and 0.7 at the beginning of the experiments also indicate functional, intact zooxanthellae. The abrupt decrease of the values on starvation day 1 was due to an accidental overexposure of the animal to high irradiances on the same day. The following increase of the values proves intact zooxanthellae that are able to recover from this stress situation (Fig. 9). Similar effects have been observed in *P. briareum* (Burghardt *et al*., 2005), *P. colemani* (unpublished data) and *P. rudmani* (Burghardt & Gosliner, 2006). The slope of the photosynthesis *vs* irradiance curves (P–E curves) additionally gives an evidence for functional chloroplasts inside the zooxanthellae of *P. lembehensis* n. sp. (Fig. 10C). The light saturation index (E_k) of this species is comparably high (see Table 3). This might either be due to a different strain or ecotype of *Symbiodinium* that is adapted to higher irradiances than the ones of *P. lizardensis* n. sp., *P. jakobsenae* and *P. rudmani* or to acclimation of the same strain/ecotype to higher irradiances. Additionally, we cannot completely exclude that different physiological conditions inside the different slug species influence the data on the photosynthesis of zooxanthellae.

The fact that all *Phyllodesmium* species associated with members of the Xeniidae are only found on their food coral does not necessarily prove that they still depend on their food source, as suggested by Rudman (1991). This has already been discussed by Burghardt & Wägele (2004) for *P. jakobsenae* and by Burghardt & Gosliner (2006) for *P. rudmani*. Specimens of other species with a cryptic appearance and well-established symbiosis (e.g. *P. briareum*; Rudman, 1991; Burghardt, Stemmer & Wägele, 2008) are also mainly observed on their food coral. Remaining on the home coral at least provides shelter due to camouflage in colour and shape.

For *Phyllodesmium koehleri* sp. nov., only histological data on the symbiosis with zooxanthellae are available. All the results on shape of cerata and branching pattern of digestive gland, with increase of light availability for the numerous zooxanthellae in the epithelium, indicate an established mutualistic symbiotic relationship. Nevertheless, long-term starvation experiments with measurements of the photosynthetic activity of the involved zooxanthellae inside *P. koehleri* n. sp. are needed.

These studies here, compared with those recently published (Burghardt & Wägele, 2004; Wägele, 2004; Burghardt & Gosliner, 2006; Burghardt, Stemmer & Wägele, 2008), indicate interspecific differences in the mutualistic symbosis in the genus *Phyllodesmium*. Due to several morphological adaptations which support the long-term retention of zooxanthellae in varying ways, different efficiencies could be observed. Future phylogenetic analyses will help to understand these different evolutionary traits.

ACKNOWLEDGEMENTS

We would like to thank our diving and collecting companions on Lizard Island and in Lembeh Strait: Michael Berumen (Woods Hole), Rosana Carvalho-Schrödl, Enrico Schwabe and Dirk Eheberg (Munich), Kristina Stemmer and Verena Vonnemann (Bochum). Our special thanks go to the staff of the Faculty of Fisheries & Marine Science at the Sam Ratulangi University, Manado (Sulawesi, Indonesia), especially to Gustaf Mamangkey, Fontje Kaligis and Grevo Gerung and to the directors of the Lizard Island Research Station (LIRS), Anne Hoggett and Lyle Vail for their support and creating a friendly atmosphere at this station. Special thanks also go to Erwin Köhler (Darmstadt), who kindly collected *Phyllodesmium koehleri* n. sp. Gary Cobb (Gold Coast), and Roberto Sozzani (Milan), who kindly provided the slides for Fig. 2E and F. Furthermore we would like to thank the Bunaken Island National Park Authority for successful cooperation. We also thank Claudia Brefeld and Gabi Strieso (Bochum) for preparing histological sections and helping with scanning electron microscopy (SEM). We would like to thank Phil Alderslade (Darwin) for helping with identification of soft corals.

FUNDING

This study was funded by the German Science Foundation to Heike Wägele (SSP 1127 "Adaptive Radiation - Origin of Biological Diversity": Wa 618/8) and to Michael Schrödl (Schr 667-3). The GeoBioCenter (Munich) supported travel funds to Michael Schrödl.

REFERENCES

AVILA, C., BALLESTEROS, M., SLATTERY, M. & PAUL, V.J. 1998. *Phyllodesmium guamensis* (Nudibranchia, Aeolidoidea), a new species from Guam (Micronesia). *Journal of Molluscan Studies*, **64**: 147–160.

BABA, K. 1949. *Opisthobranchia of Sagami Bay collected by His Majesty The Emperor of Japan*. Iwanami Shoten, Tokyo.

BABA, K. 1991. Taxonomical study on some species of the genus *Phyllodesmium* from Cape Muroto-misaki, Shikoku and Okinawa Province, Southern Japan (Nudibranchia: Facelinidae). *Venus*, **50**: 109–123.

BARRETT, J. & BARRETT, D. 2004. *Phyllodesmium* sp. 2 from New Britain. *Sea Slug Forum*, *http://seaslugforum.net/display.cfm?id=12307*.

BERGH, L.S.R. 1896. Eolidiens D'Amboine. Voyage de MM. M. Bedot et C. Pictet dans l'Archipel Malais. *Revue Suisse de Zoologie et Annales de Musée d'Histoire Naturelle de Genève*, **4**: 385–394.

BERGH, L.S.R. 1905. Die Opisthobranchiata der Siboga-Expedition. *Siboga epeditie*, **50**: 1–248.

BOLLAND, R.F. 2005. *Phyllodesmium* sp. 1. *Okinawa Slug Site*, http://rfbolland.com/okislugs/phyl_sp.1.html.

BURGHARDT, I., EVERTSEN, J., JOHNSEN, G. & WÄGELE, H. 2005. Solar powered seaslugs – mutualistic symbiosis of aeolid Nudibranchia (Mollusca, Gastropoda, Opisthobranchia) with *Symbiodinium*. *Symbiosis*, **38**: 227–250.

BURGHARDT, I. & GOSLINER, T.M. 2006. *Phyllodesmium rudmani* (Mollusca: Nudibranchia: Aeolidoidea), a new solar powered species from the Indo-West Pacific with data on its symbiosis with zooxanthellae. *Zootaxa*, **1308**: 31–47.

BURGHARDT, I., STEMMER, K. & WÄGELE, H. 2008. Symbiosis between *Symbiodinium* (Dinophyceae) and different taxa of Nudibranchia (Mollusca: Gastropoda) with analyses of longterm retention. *Organisms, Diversity and Evolution*, **8**: 66–76.

BURGHARDT, I. & WÄGELE, H. 2004. A new solar powered species of the genus *Phyllodesmium* Ehrenberg, 1831 (Mollusca: Nudibranchia: Aeolidoidea) from Indonesia with analysis of its photosynthetic activity and notes on biology. *Zootaxa*, **596**: 1–18.

BURGHARDT, I. & WÄGELE, H. 2006. Interspecific differences in the efficiency and photosynthetic characteristics of the symbiosis of "solarpowered" Nudibranchia (Mollusca: Gastropoda) with zooxanthellae. *Records of the Western Australian Museum*, Supplement **69**: 1–9.

BURN, R. 1962. Descriptions of Victorian nudibranchiate Mollusca, with a comprehensive review of the Eolidacea. *Memoirs of the National Museum*, **25**: 95–128.

COBB, G. 2004 (December 5). *Phyllodesmium* sp. 3. *Opisthobranchs of the Sunshine Coast*, http://www.nudibranch.com.au/pages/7928b.htm.

EHRENBERG, G.G. 1831. *Symbolae Physicae seu icones est descriptiones animalium evertebratorum sepositis insectis quae ex itinere per Agricam Borealem et Asiam Occidentalem*. Decas 1 Mollusca.

MACNAE, W. 1954. On some aeolidacean nudibranchiate molluscs from South Africa. *Annals of the Natal Museum*, **13**: 1–50.

ORTIZ, D.M. & GOSLINER, T.M. 2003. A New Species of *Phyllodesmium* Ehrenberg, 1831 (Mollusca, Nudibranchia) from the Tropical Indo-Pacific. *Proceedings of the California Academy of Sciences*, **54**: 161–168.

RUDMAN, W.B. 1981. The anatomy and biology of alcyonarian-feeding on aeolid opisthobranch molluscs and their development of a symbiosis with zooxanthellae. *Zoological Journal of the Linnean Society, London*, **72**: 219–262.

RUDMAN, W.B. 1991. Further studies on the taxonomy and biology of the octocoral-feeding genus *Phyllodesmium* Ehrenberg, 1831 (Nudibranchia, Aeolidacea). *Journal of Molluscan Studies*, **57**: 167–203.

SOZZANI, R. 2004. *Phyllodesmium* sp. 2 from Indonesia. *Sea Slug Forum*, http://www.seaslugforum.net/display.cfm?id=12313.

WÄGELE, H. 2004. Potential key characters in Opisthobranchia (Gastropoda, Mollusca) enhancing adaptive radiation. *Organisms, Diversity and Evolution*, **4**: 175–188.

WÄGELE, H., BURGHARDT, I., ANTHES, N., EVERTSEN, J., KLUSSMANN-KOLB, A. & BRODIE, G. 2006. Species diversity of opisthobranch molluscs on Lizard Island, Great Barrier Reef, Australia. *Records of the Western Australian Museum, Supplement* **69**: 33–59.

WÄGELE, H. & JOHNSEN, G. 2001. Observations on the histology and photosynthetic performance of "solar-powered" opisthobranchs (Mollusca, Gastropoda, Opisthobranchia) containing symbiotic chloroplasts or zooxanthellae. *Organisms, Diversity and Evolution*, **1**: 193–210.

WEBB, W. L, NEWTON, M. & STARR, D. 1974. Carbon dioxide exchange of *Alnus rubra*: a mathematical model. *Oecologia*, **17**: 281–291.